Infrared image detail enhancement based on local adaptive gamma correction

Bin Liu (刘 斌), Xia Wang (王 霞)*, Weiqi Jin (金伟其), Yan Chen (陈 艳), Chongliang Liu (刘崇亮), and Xiu Liu (刘 秀)

Key Laboratory of Photoelectronic Imaging Technology and System (Beijing Institute of Technology), Ministry of Education, School of Optoelectronics, Beijing Institute of Technology, Beijing 100081, China

**Corresponding author: angelniuniu@bit.edu.cn*

Received April 7, 2011; accepted July 8, 2011; posted online September 2, 2011

An infrared image detail enhancement method based on local adaptive gamma correction (LAGC) is proposed. The local adaptive gamma values are designed based on the Weber curve to enhance effectively the image details. Subsequently, the active grayscale range of the image processed by LAGC is further extended by using our proposed histogram statistical stretching. The experimental results show that the proposed algorithm could considerably increase the image details and improve the contrast of the entire image. Thus, it has significant potential for practical applications.

OCIS codes: 100.2980, 100.2000, 110.3080.
doi: 10.3788/COL201210.021002.

An infrared (IR) image generally represents the IR radiation of a scene. From the macro point of view, temperatures at different positions in the scene could vary considerably. However, on the surface of certain objects, the temperatures at adjacent spatial and temporal positions are highly correlated. Therefore, the acquired IR images typically show high dynamic range (HDR) and low temperature resolution. To preserve well the significant details of the IR scene, high-precision analog/digital converter (ADC, 12 or 14 bit) embedded in the IR camera is needed. On the other hand, normal monitor could only display 8-bit images. To address the limitation of the normal monitor, the 14-bit data from ADC must be compressed into 8-bit data, and in the process, some significant details could be lost. This situation could seriously restrict the applications of IR imaging systems. Therefore, the main focus of this letter is the process that can achieve effective compression of the HDR and perfect preservation of the image details.

The traditional gamma correction, a kind of widely used contrast enhancement, was very popular owing to its simplicity and ease of handling in real-time systems[1]. It improves image contrast through a specified gamma correction curve. Another kind of widely used contrast enhancement is the histogram equalization (HE)-based method. It can be categorized into two types, namely, the global HE (GHE) and the local HE (LHE). The fundamental of the GHE-based methods is to distribute equally the probability distribution function (PDF) of the resulting image on the full grayscale range. Therefore, high-PDF grayscales could be dramatically enhanced. However, the low-PDF grayscales, which generally represented significant details, were suppressed or even lost during HE processing[2]. The plateau equalization, contrast limited adaptive HE (CLAHE), and brightness preserving bi-histogram equalization are variations of the traditional GHE[3−5]. LHE is a method that applies HE processing in the local regions[6]. Although the image quality processed by LHE is superior to GHE, its practical application remains limited owing to its high computational expense and complexity. Recently, a novel contrast enhancement, called partially overlapped sub-block HE (POSHE), was presented[7]. It is capable of highlighting the local details, as well as dramatic reduction of computational time. In addition to the aforementioned enhancement methods, numerous other kinds of contrast enhancements were proposed, such as unsharp masking, retinex-based enhancement, wavelet processing, and nature-firing intersecting cortical model[8−10]. Recently the FLIR Company equipped its high-performance IR systems with a digital detail enhancement technique[11]. The technique enables IR systems not only to improve image contrast but also highlight significant local details in the scene, consequently enhancing the performance of IR systems.

To observe the image details better, human visual properties should be incorporated in the design of the detail enhancement. Thus, in this letter, by using the Weber curve, the IR image detail enhancement based on local adaptive gamma correction (LAGC) is proposed to satisfy human observation.

The traditional gamma correction can be formulated as

$$r(i,j) = (2^N - 1) * \left[\frac{o(i,j)}{2^M - 1}\right]^{\gamma}, \tag{1}$$

where $o(i,j)$ represents the original input image, $r(i,j)$ represents the gamma-corrected output, γ is the correction parameter, and M and N are the digits of input and output images, respectively. To preserve the details of the IR scene better, we use a high-precision digital output from an IR camera as input of this algorithm. M is generally equal to 14 bit, and N is equal to 8 bit to accommodate the function of normal monitors.

The correction curves of different γ are shown in Fig. 1. When dealing with practical IR images, the traditional gamma correction involves two problems: 1) the expected visual perception of the output image highly relies on manual settings, and only experts can provide the proper gamma value; 2) the traditional gamma correction is a

global method with different grayscales sharing the same correction curve. Thus, local details cannot be effectively enhanced at the same time.

The key objective of LAGC therefore, is how to acquire the proper local adaptive gamma values based on the aforementioned analysis.

Research on human visual system shows that human visual response to brightness difference on different backgrounds varies dramatically[12]. However, in a certain range, the ratio between the discernable difference and the background is constant, i.e., the Weber ratio[1]. We define

$$\frac{\Delta I}{I} = K, \tag{2}$$

$$\lg(\Delta I) = \lg(K) + \lg(I), \tag{3}$$

where I is the background and ΔI is the discernable difference, called just noticeable difference (JND); K is the Weber ratio representing the visual capability to distinguish brightness difference. The Weber curve is shown in Fig. 2[1]. In the Weber's law range, the logarithm of the discernable difference is nearly proportional to the logarithm of the background. However, in the dark-light range, JND remains constant as the background brightness decreases, that is, the K value increases. This fact shows that the human visual response to JND in dark light is highly inadequate. In the saturation range, the JND greatly increases as the background brightness increases, indicating that the slope of the curve in this range is very steep. Therefore, the K value also increases.

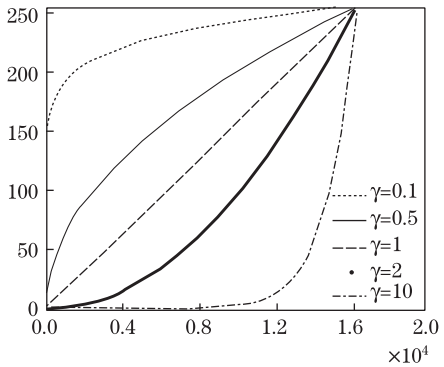

Fig. 1. Gamma correction curves.

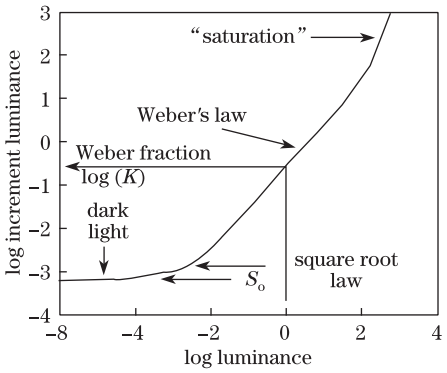

Fig. 2. Weber curve for discernable luminance difference.

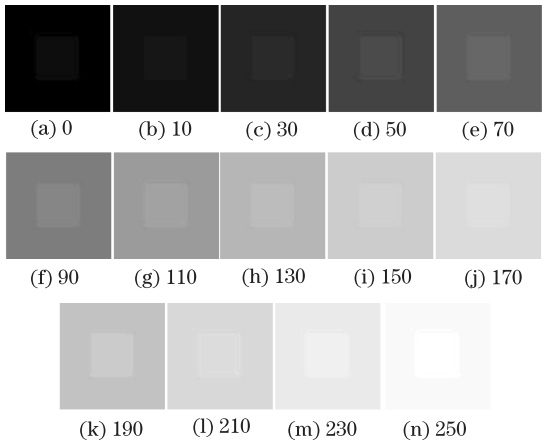

Fig. 3. Simulated images of same grayscale difference on different grayscale backgrounds.

This fact shows that the human visual response to the JND in this range is also poor.

In reality, human eyes can only differentiate approximately 50 grayscales. In Fig. 3, we simulate a group of images in which the different backgrounds are accompanied with objects with the same gray difference (ΔI=5). The gray values of the backgrounds are 0, 10, 30, 50, 70, 90, 110, 130, 150, 170, 190, 210, 230, and 250, as shown in Figs. 3(a)–(n). From these images, the objects can be hardly seen against the darker and brighter backgrounds. However, in the middle backgrounds, we can easily observe the objects. Hence, we should design the detail enhancement algorithm according to the Weber curve to ensure that the enhanced details can be successfully perceived against different backgrounds.

Based on the above discussions, we should provide higher K values in the darker and brighter backgrounds. However, in practical high-precision image data, the active grayscale range is ordinarily narrow. To take full advantage of the entire grayscale range and make sure the background intensity significantly varies, we perform linear extension of the active grayscales as first procedure.

$$o'(i,j) = \frac{(2^M - 1)[o(i,j) - o_{\min}]}{o_{\max} - o_{\min}}, \tag{4}$$

where $o'(i,j)$ denotes the linearly adjusted image data; $o_{\max}$ and $o_{\min}$ are the maximum and minimum values of $o(i,j)$, respectively.

By fitting the Weber curve, we design the local adaptive gamma value as

$$\gamma(i,j) = \exp\left[\frac{l(i,j) - 2^{M-1}}{2^{M-1}}\right], \tag{5}$$

where $l(i,\ j)$ is the low-pass filtering result of $o'(i,j)$, and its values represent the mild background. To protect the sharp edges in the image, we utilize a 5×5 bilateral filter to implement low-pass filtering[13].

When the background is less than 2^{M-1}, γ is smaller than 1. As can be observed in Fig. 1, the difference between the object and the background is considerably magnified, which meets the purpose of providing a higher K in the darker range. When the background is more

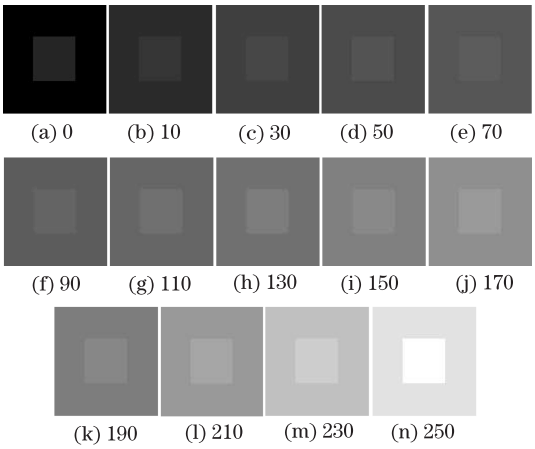

Fig. 4. Adaptive gamma correction results of Fig. 3.

than 2^{M-1}, γ is greater than 1, and the difference would also be significantly magnified in the brighter range. Figure 4 shows the results of Fig. 3 after LAGC processing. In addition to Figs. 4(c)–(m), the objects can be observed in Figs. 4(a), (b), and (n). However the objects can hardly be seen in Figs. 3(a), (b), and (n). The final formula of the proposed algorithm can be expressed as

$$r(i,j) = (2^N - 1) * \left[\frac{o'(i,j)}{2^M - 1}\right]^{\exp[\frac{l(i,j)-2^{M-1}}{2^{M-1}}]}. \quad (6)$$

When the residual bad pixels exist in the IR images, the gray values enhanced by LAGC are usually assembled in a limited grayscale range. To extend the active grayscale range further, we present the histogram statistical stretching (HSS) processing to explore the image details. The processing steps are as follows.

1) Calculation of the histogram of the image processed by LAGC

$$g_{\max} = p(h_{\mathrm{LAGC}}, p_{\max}), \quad (7)$$

where h_{LAGC} is the histogram of the image processed by Eq. (6); $p(x, y)$ is the function used to find the position of y in the sequence of x; $p_{\max}$ is the maximum PDF in the histogram; $g_{\max}$ is the corresponding position of $p_{\max}$ in the histogram.

2) Summing up of the PDFs from both sides of $g_{\max}$ in an interlaced manner

$$h_{\mathrm{sum}} = \sum_{k=g_{\max}-m}^{g_{\max}+m} \quad p_r(k) = \sum_{k=g_{\max}-m}^{g_{\max}+m} \frac{n_k}{n},$$

$$\text{if } \max(h_{\mathrm{sum}}) \leqslant v_{\mathrm{t}} \quad m = 0, 1, 2, \cdots 2^N - 1, \quad (8)$$

where $p_{\mathrm{r}}(k) = n_k/n$ is the PDF of the kth gray level; n_k and n are the pixels of the kth gray level and the total pixels, respectively; m represents the distance far from $g_{\max}$; h_{sum} is the result of PDF summing up; $\max(x)$ is the function used to find the maximum value in the sequence of x; v_t is the threshold that we manually set in the formula to halt the cumulative process. The process can be categorized into two situations.

a) Normal situation: if the threshold is achieved, then $v_{\min} = g_{\max} - m$ and $v_{\max} = g_{\max} + m$.

b) Abnormal situation: if the PDF of $g_{\max} - m$ approaches zero, then $v_{\min} = g_{\max} - m$. Subsequently, the gray levels greater than $g_{\max}$ are only summed in the cumulative process until the threshold is achieved, and $v_{\max} = g_{\max} + m'$, or vice versa.

(3) Execution of the histogram stretching to accommodate the grayscale range of the normal monitor

$$q(k) = \begin{cases} 0 & \text{if} \quad k < v_{\min} \\ 2^8 - 1 & \text{if} \quad k > v_{\max} \\ \dfrac{(2^8 - 1)(k - v_{\min})}{v_{\max} - v_{\min}} & \text{otherwise} \end{cases}, \quad (9)$$

where $q(k)$ represents the mapping function from the input to the output. After HSS processing, the active grayscale range could be extended further, and the details enhanced by LAGC will clearly show up.

Figures 5–7 show the practical mid-wave IR and near-IR (NIR) images processed by LAGC–HSS. The parameter v_t used in these experiments is equal to 0.98. To show the performance of LAGC–HSS better, we compare it with the traditional gamma correction, automatic gain control (AGC), GHE, and POSHE.

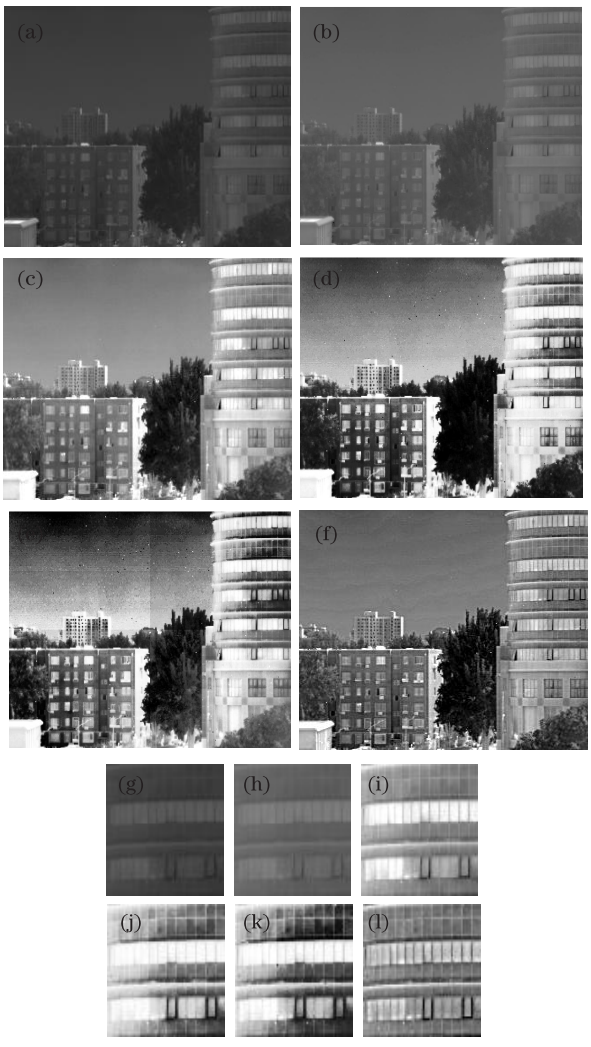

Fig. 5. Experimental results of the sky-terrain scene. (a) Original image; (b) γ correction (γ=0.7); (c) AGC; (d) GHE; (e) POSHE; (f) LAGC-HSS; (g)–(l) local regions of (a)–(f).

Figure 5(a) shows the original HDR image (14 bit), which has a narrow active grayscale range and low contrast because of overheated objects and few residual bad pixels existing in the image. Figure 5(b) shows the result obtained by traditional gamma correction ($\gamma = 0.7$). The entire brightness of the image is upgraded. The details, nevertheless, are not enhanced. AGC is shown in Fig. 5(c). Compared with that shown in Fig. 5(b), the active grayscale range is much improved, and the contrast is better. Figures 5(d) and (e) show the GHE and POSHE results, respectively. As mentioned earlier, GHE could enhance the contrast of high-PDF grayscales and suppress the contrast of low-PDF ones. In the results, the contrast of the sky and building is effectively improved. However, the unnatural wash-out effect is also obvious, leading to a poor perception of the image details. In contrast to the previous four results, the image enhanced by LAGC–HSS shown in Fig. 5(f) has the most discernable details and the best rational dynamic range. In particular, the building surface, which was insufficiently enhanced by the previous methods, is shown clearly in Fig. 5(f). The local regions in Figs. 5(a)–(f) are shown in Fig. 5(g)–(l), respectively. By comparing the magnified local regions, we find that the details processed by LAGC–HSS are the best.

Figure 6(a) shows another HDR image (14 bit) of the flame scene where the flame is located on the left side of the image. Compared with the rest of the parts of the IR scene, the flame is overheated and occupies a major part. Therefore, the traditional gamma correction and AGC could not acquire good visual results. The wash-out effect generated by GHE and POSHE negatively affects human perception of the image texture. For example, the structures of the building on the left cannot be clearly observed. Figure 6(f) shows the image enhanced by LAGC–HSS. Most of the discernable details of the scene are displayed. The structures of the buildings on the left and right sides and the tree branches in the middle can all be observed.

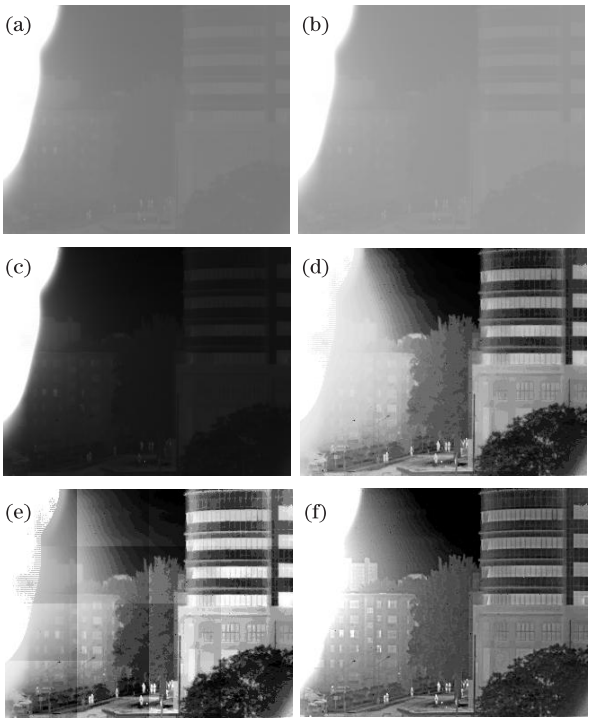

Fig. 6. Experimental results of the flame scene. (a) Original image; (b) γ correction ($\gamma = 0.7$); (c) AGC; (d) GHE; (e) POSHE; (f) LAGC-HSS.

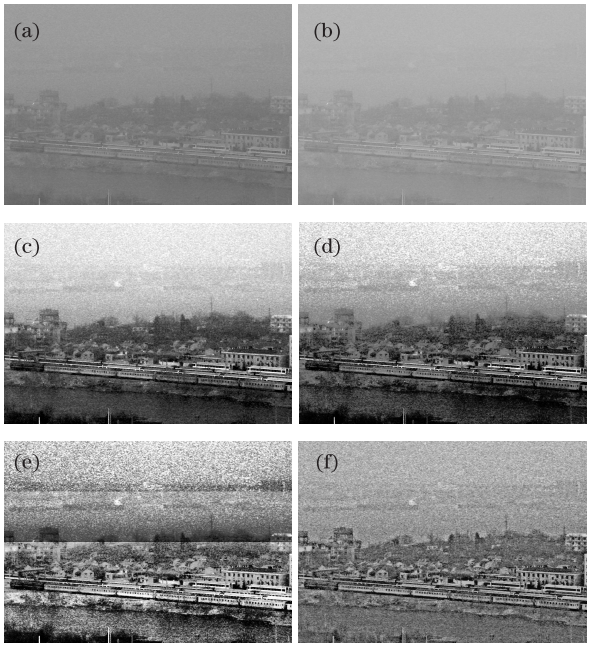

Fig. 7. Experimental results of the NIR image with mass fog. (a) Original image; (b) γ correction ($\gamma = 0.7$); (c) AGC; (d) GHE; (e) POSHE; (f) LAGC-HSS.

Figure 7(a) shows a low dynamic range NIR image (8 bit) due to the mass fog within the scene. The traditional gamma correction and AGC could improve the image contrast to a certain degree, whereas GHE and POSHE can extremely enhance the background, which can result in the loss of some significant details. The image enhanced by LAGC–HSS shows the most number of details we deem important in the scene.

Entropy is sometimes considered as a criterion to assess the performance of image enhancement. However, it is not suitable enough to assess comprehensively the real performance. In 2007, Agaian *et al.* proposed the new evaluation of enhancement (EME) to assess quantitatively the enhancement performance[14]. EME approximates the average contrast in images by partitioning the image into non-overlapping blocks, finding a measure based on the minimum and maximum gray values in each block, and averaging them to generate the final value. The EME value represents the degree of local changes. If more details exist in the image, then the value of EME will be larger. The EME values derived from Figs. 5–7 are listed in Table 1, where we note that the original image has a narrow active grayscale range and poor detail perception; therefore, its EME value is small. In the traditional gamma correction, the details are not effectively enhanced, and the dynamic range is suppressed as well. Thus, its EME value is smaller than that of the original image. AGC could extend the active grayscale range and improve the details; thus, its EME value is superior to that of the original image. With GHE and POSHE, considered as two kinds of effective enhancement methods, the EME values are greater

Table 1. EME Evaluations

	Original Image	γ Correction	AGC	GHE	POSHE	LAGC-HSS
Fig. 5	15.6353	12.0617	54.6616	84.8430	103.1200	143.6750
Fig. 6	2.681	1.881	19.707	58.559	106.404	120.008
Fig. 7	7.288	5.107	49.026	70.939	147.139	153.532

than those of the original image and those derived by the AGC method. POSHE is capable of highlighting the local details. Therefore, in concept, POSHE is better than GHE. Compared with these methods, LAGC–HSS can obtain the largest EME value, which can produce the best details in the image.

The subjective and objective evaluations verify that LAGC–HSS is capable of compressing sufficiently the HDR image and enhancing the image details effectively. Consequently, it could improve the human perception of the IR scene considerably.

In conclusion, we present an effective detail enhancement method that is especially suitable for the HDR IR image, based on human visual property. In contrast to the traditional gamma correction, LAGC–HSS has the ability to update adaptively the gamma values with respect to the local regions. Moreover, it can effectively extend the active grayscale range after LAGC processing, by using the proposed HSS. The experiments prove that the image enhanced by LAGC–HSS shows the perfect natural appearance with more readily perceptible details. In addition, the example of a NIR image with mass fog within the scene proves that this algorithm can also be used in haze-removal applications. Based on these, the algorithmic optimization and implementation on the real-time system will be our main topic for study in the future.

This work was supported in part by the National Natural Science Foundation of China (Nos. 60877060 and 60971010) and the Research Fund for the Doctoral Program of Higher Education of China (No. 20070007022).

References

1. R. C. Gonzalez and R. E. Woods, *Digital Image Processing* (2nd Edition) (Prentice Hall, New Jersey, 2003).
2. T. Arici, S. Dikbas, and Y. Altunbasak, IEEE Trans. Image Proc. **18,** 1921 (2009).
3. V. E. Vickers, Opt. Eng. **35,** 1921 (1996).
4. C. Lu, H. Hsu, and L. Wang, in *Proceedings of 2009 IEEE International Workshop on Imaging Systems and Technique* 407 (2009).
5. Y. Kim, IEEE Trans. Consum. Electron. **43,** 1 (1997).
6. K. Kokufuta and T. Maruyama, in *Proceedings of International Conference on Field Programmable Logic and Applications* 288 (2009).
7. J. Kim, L. Kim, and S. Hwang, IEEE Trans. Circ. Syst. Video Technol. **11,** 475 (2001).
8. A. Polesel, G. Ramponi, and V. J. Mathews, IEEE Trans. Image Proc. **9,** 505 (2000).
9. C. Li, S. Gao, and D. Bi, Chin. Opt. Lett. **7,** 784 (2009).
10. S. Gao, C. Li, and D. Bi, Chin. Opt. Lett. **8,** 474 (2010).
11. "Digital Detail Enhancement. Technical Note" http:// www.flir.com/ uploadedfiles/Eurasia /MMC/Tech_Notes.
12. T. Yu, Q. Li, and J. Dai, Chin. Opt. Lett. **7,** 206 (2009).
13. S. Paris, P. Kornprobst, J. Tumblin, and F. Durand, Foundations and Trends® in Computer Graphics and Vision **4,** 1 (2008).
14. S. S. Agaian, B. Silver, and K. A. Panetta, IEEE Trans. Image Proc. **16,** 741 (2007).